

Performance of Borel-Laplace integrator for the resolution of stiff and non-stiff problems

Ahmad Deeb¹, Aziz Hamdouni², and Dina Razafindralandy*³

¹ahmad.deeb@univ-lr.fr

²aziz.hamdouni@univ-lr.fr

³dina.razafindralandy@univ-lr.fr

Laboratoire des Sciences de l'Ingénieur pour l'Environnement
 LaSIE, UMR-7356-CNRS, La Rochelle Université
 Avenue Michel Crépeau, 17042 La Rochelle Cedex 1, France

Abstract

A stability analysis of the Borel-Laplace series summation technique, used as explicit time integrator, is carried out. Its numerical performance on stiff and non-stiff problems is analyzed. Applications to ordinary and partial differential equations are presented. The results are compared with those of many popular schemes designed for stiff and non-stiff equations.

1 Introduction

Stiff problems occur in many areas of engineer science, such as mechanics, electrical and chemical engineering (see for instance [1, 2, 3, 4]). However, their resolution has remained a challenge for numerical analysts. The reason is that many numerical methods designed for general ordinary differential equations exhibit a high instability when solving stiff problems, unless an excessively small time step is used. As a consequence, numerical schemes with better stability properties have been developed especially for stiff problems.

One method used to estimate the biggest time step allowed by a given numerical scheme without breaking its stability is the analysis of the linear stability domain. The scheme is called *A*-stable if this domain contains the half complex plane with negative real part, meaning that the scheme is stable in some sense however big is the time step, for the resolution of a 1D linear equation. The notions of linear stability domain will be recalled later. See also [1, 4] for different notions of stability. Of course, even if a scheme is *A*-stable, the time step is limited in practice due to precision requirements.

*Corresponding author

One of the most widely used numerical schemes for stiff equations are the implicit linear multistep methods based on backward difference formulas (BDF). Their stability are limited to low orders. Indeed, only the first order (implicit Euler) and the second order are A -stable. BDF of order 3 to 6 exhibit a weaker stability property which is the $A(\alpha)$ -stability, and the formulas of order bigger than 6 are unstable. A generalization of BDF which uses a second derivative permits to obtain implicit $A(\alpha)$ -stable schemes up to order 10.

Another important family of numerical schemes for differential equations are Runge-Kutta methods (RK). Compared to multistep methods, it is easier to find stable implicit Runge-Kutta schemes. For example, Gauss, Radau IA and IIA, and Lobatto IIIA, IIIB and IIIC are A -stable.

Of course, there are some other schemes suitable for stiff problems. A common point of all the cited algorithms is their implicit character. Indeed, no explicit method in the family of BDF or RK schemes is A -stable. However, the cost of an implicit scheme may be very high. This is particularly true for fast dynamic problems (damage mechanics, molecular dynamics, ...) where the use of implicit methods is not conceivable. The development of explicit, yet with a good enough stability property, numerical schemes is desirable.

An approach which has been used to this aim is to build stabilized RK schemes [1, 5]. These schemes are not A -stable like the implicit RK schemes but have a larger stability domain than standard explicit RK schemes.

Other semi-explicit schemes which are built for stiff problems are exponential time differencing (ETD) integrators. They are based on an exact, exponential type, resolution of the linear part of the equation. In doing so, the stiff part of the solution is correctly captured if it is an exponentially decaying term. The complete solution, the expression of which can be found by the variation of constants method, is then computed numerically. Various schemes have been proposed for this tasks [6, 7, 8, 9, 10, 11]. One of the most popular exponential integrators is the exponential time differencing associated to an explicit 4-th order Runge-Kutta method (ETDRK4) developed by Cox and Matthews [12]. The algorithm is not completely explicit since it requires the (pseudo-)inversion of a matrix. Moreover, they generally need the evaluation of the exponential of a matrix, which is numerically expensive.

In the present article, we examine the performance of the Borel-Laplace integrator (BL) in solving stiff and non-stiff systems. BL is an entirely explicit, arbitrary high-order scheme. It is based on a decomposition of the solution into its time Taylor series, followed by a Borel-Laplace summation procedure to accelerate the convergence, or in the case of a divergent series, to obtain an asymptotical solution. The first goal of the article is the study of the stability of BL. We will see that, although not A -stable (as most of explicit methods), BL admits a stability region which grows very fast with the order of the scheme. This enables big time steps compared to many popular explicit and even implicit schemes in practice. The second goal of the article is to show that BL is suited to the resolution of stiff equations and to problems with high degree of freedom.

At its origin, the Borel-Laplace summation method was intended to define the asymptotic sum of a Gevrey series, that is a series which does not

diverge faster than a series of factorials [13]. It has recently gained more interest when authors showed that many equations in mechanics (heat, Burgers and Navier-Stokes equations, ...), quantum physics or astronomy have divergent but Gevrey Taylor series [14, 15, 16, 17, 18, 19]. The Borel-Laplace summation method has been transformed into numerical algorithm [20] and used for the first time as a time integrator by Razafindralandy and Hamdouni [21]. Since then, many qualities of the Borel-Laplace integrator was found. For example, it generally allows much bigger time steps than other explicit methods for the resolution of many problems [21]. Its ability to cross some types of singularities, its high-order symplecticity, or its high-order iso-spectrality in solving a Lax pair problem have been stated in [22]. Another advantage of BL is that lowering or raising the approximation order is as simple as changing the value of a parameter in the code. However, nowhere in the cited works on the Borel-Laplace integrator stiffness has been addressed. One aim of the present article, as mentioned, is to fill this gap.

The Borel-Laplace algorithm that will be discussed here results from the representation of the Borel sum as a Laplace integral. A representation as a factorial series also leads to an efficient algorithm [23] but will not be used.

This paper is organized as follows. In section 2, the Borel-Laplace algorithm is briefly recalled. In section 3, a linear stability analysis is carried out. The stability regions, corresponding to different values of parameters, are plotted. In section 4, numerical performance on stiff and non-stiff ODE problems as well as on a PDE is analyzed.

2 Borel-Laplace integrator

Consider an ordinary differential equation or a semi-discretized partial differential equation :

$$\begin{cases} \frac{du}{dt} = F(t, u), \\ u(t = 0) = u_0, \end{cases} \quad (1)$$

where

$$\begin{aligned} u : [0, T] &\longrightarrow \mathbb{R}^n \\ t &\longmapsto u(t) \end{aligned}$$

is the unknown, $n \in \mathbb{N}$ is the dimension of the system. F is a non-linear operator

$$\begin{aligned} F : \mathbb{R} \times \mathbb{R}^n &\longrightarrow \mathbb{R}^n \\ (t, v) &\longmapsto F(t, v). \end{aligned}$$

Borel-Laplace integrator consists in finding the solution of (1) as a (convergent or divergent) time series

$$u(t) = \sum_{k=0}^{\infty} u_k t^k \in (\mathbb{C}[t])^n \quad (2)$$

and performing a Borel-Laplace summation procedure on this series. To simplify, assume that $n = 1$. The terms u_k are obtained by injecting directly the series expansion (2) in equation (1). This leads to explicit relations of the form

$$u_{k+1} = \frac{1}{k+1} F_k(u_0, \dots, u_k) \quad (3)$$

where F_k is the k -th Taylor coefficient of $F(t, u(t))$ at $t = 0$. It is generally a non-linear function of u_0, u_1, \dots, u_k . The expression of F_k will be explicitly given for each equation we will be dealing with.

The (exact or numerical) radius of convergence of series (2) may be zero. In this case, a summation procedure is necessary. The one chosen here is the Borel-Laplace summation. When radius of convergence is not zero, the summation is optional but is systematically used since it enlarges the domain of validity of the series and makes the calculations faster. As will also be seen later, it extends the stability region.

2.1 Computational aspect of Borel-Laplace summation

The theory behind Borel-Laplace summation can be found in many papers [13, 24, 25, 26] and shall not be reproduced here. Only the computation aspect is presented. Let us assume that series (2) is a p -Gevrey series, that is,

$$|u_k| \leq CA^k(k!)^p, \quad \forall k \geq 0 \quad (4)$$

for some positive real numbers A and C . In fact, it is known that most of series arising in engineering problems are p -Gevrey series for some positive rational number p . In the sequel, we consider only the case $p = 1$.

The summation is done in three stages. First, the Borel transform

$$\mathcal{B}\hat{u}(\xi) = \sum_{k=0}^{\infty} \frac{u_{k+1}}{k!} \xi^k \in \mathbb{C}[\xi] \quad (5)$$

is computed. This series is convergent at the origin. Next, $\mathcal{B}u(\xi)$ is prolonged analytically in the vicinity of a semi-line ℓ of the complex plane, linking 0 to ∞ . Lastly, the Laplace transform (at $1/t$), which is the formal inverse of the Borel transform, is applied to the prolonged function. These stages are summarized in Table 1.

If the initial series (2) is convergent at the origin, then the Borel sum $\mathcal{S}\hat{u}(t)$ obtained at the end of the procedure is the usual sum, for t inside the disc of convergence. However, the domain of definition of $\mathcal{S}\hat{u}$ is generally larger than the disc of convergence of the series \hat{u} . If the initial series is a divergent but Gevrey series, $\mathcal{S}\hat{u}$ is a sectorially analytical function, having the series \hat{u} as Gevrey asymptotics.

$$\begin{array}{ccc}
\hat{u}(t) = \sum_{k=0}^{\infty} u_k t^k & \sim & \mathcal{S}\hat{u}(t) = u_0 + \int_{\ell} P(\xi) e^{-\xi/t} d\xi \\
\text{Borel} \downarrow & & \uparrow \text{Laplace} \\
\mathcal{B}\hat{u}(\xi) = \sum_{k=0}^{\infty} \frac{u_{k+1}}{k!} \xi^k & \xrightarrow{\text{Prolongation}} & P(\xi)
\end{array}$$

Table 1: Borel-Laplace summation

2.2 Algorithm

Numerically, only a finite number of terms u_k can be computed. The series is then represented by a K -th degree polynomial

$$\hat{u}(t) \simeq u^K(t) = \sum_{k=0}^K u_k t^k.$$

The Borel transform is a $(K - 1)$ -th degree polynomial. Many techniques can be used as numerical prolongation. The one chosen here is Padé approximation [27, 28]. The algorithm will then be called Borel-Padé-Laplace integrator (BPL) in the sequel to emphasize the prolongation with Padé approximants. An usual Gauss-Laguerre quadrature permits to compute the Laplace transform [29]. In simulations, the semi-line ℓ is the positive real axis.

The cut-off order K can be assimilated as the order of the scheme. Note that one advantage of Borel-Laplace integrator is that, contrarily to many schemes such as BDF or Runge-Kutta, increasing the order is very simple. Raising K is enough; the algorithm needs not to be modified, no coefficient has to be changed.

Of course, the solution $\mathcal{S}\hat{u}(t)$ obtained with BPL is good only up to some value t_f of t . When this value is reached, the algorithm (computation of u_k 's and Borel summation) is restarted, using $\mathcal{S}\hat{u}(t_f)$ as initial condition at $t = t_f$. One way of appreciating the quality of the solution is to calculate the residue of the solution. This strategy is rather expensive but, as will be seen, is fast enough to compete with all the other numerical schemes under consideration.

The Borel-Padé-Laplace algorithm can be summarized as follows, for a one-dimensional problem, with the residue as quality criteria:

1. Start with $t_0 = 0$, $u_0 = u(t_0)$.
2. Compute the first K coefficients of the series:

$$u_{k+1} = \frac{1}{k+1} F_k(t_0, u_0, \dots, u_k), \quad k = 0, \dots, K-1$$

where F_k is the k -th Taylor coefficient of $F(t, u(t))$ at $t = t_0$.

3. Apply a Borel transformation:

$$u'_k = \frac{u_{k+1}}{k!}, \quad k = 0, \dots, K-1.$$

4. Compute the $[K_a/K_b]$ Padé approximant $P(\xi)$ of the polynomial with coefficients u'_k , *i.e.* determine a_k and b_k such that

$$u'_0 + u'_1 \xi + \dots + u'_{K-1} \xi^{K-1} + O(\xi^K) = \frac{a_0 + a_1 \xi + \dots + a_{K_a} \xi^{K_a}}{1 + b_1 \xi + \dots + b_{K_b} \xi^{K_b}} =: P(\xi).$$

5. Obtain the approximate Borel sum by computing the Laplace transform with a N_G -point Gauss-Laguerre quadrature formula¹:

$$\mathcal{S}u^K(t) = u_0 + t \sum_{i=1}^{N_G} P(t\xi_i) w_i. \quad (6)$$

6. Find t_f such that the relative residue norm is smaller than a tolerance ϵ for all $t \leq t_f$:

$$\left\| \frac{d\mathcal{S}u^K}{dt} - F(\mathcal{S}u^K) \right\| < \epsilon \|\mathcal{S}u^K\|, \quad \forall t \leq t_f.$$

Take $\mathcal{S}u^K(t)$ as the approximation of $u(t)$ for $t \in [t_0, t_f]$.

7. Return to step 2 with $t_0 = t_f$, $u_0 = \mathcal{S}u^K(t_f)$

In this algorithm, the integers K_a and K_b are such that $K_a + K_b = K - 1$. The reals ξ_i are the roots of the N_G -th Gauss-Laguerre polynomials and the w_i are the corresponding weights. The quantity $t_f - t_0$ is taken as the time step of the algorithm. Note also that an SVD decomposition will be carried out to improve the robustness of the Padé approximation in numerical tests, following an algorithm discussed in [30].

In the next section, the linear stability of BPL is analysed. In particular, a stress is put on the contribution of the summation procedure.

3 Stability analysis

Let us begin with a reminder of the notion of stability domain for an iterative scheme. Consider the linear equation

$$\begin{cases} \frac{du}{dt} = \lambda u \\ u_0 = u(t_0) \end{cases} \quad (7)$$

¹Note that $\int_0^{+\infty} P(\xi) e^{-\xi/t} d\xi = t \int_0^{+\infty} P(t\xi) e^{-\xi} d\xi$

where λ is a complex number with a negative real part. The solution of this equation decreases exponentially to zero when t grows. Consider an iterative scheme providing an approximate solution $u(t_n) \simeq v_h^n$ of (7) as follows at each iteration:

$$v_h^{n+1} = R(\lambda, h)v_h^n \quad (8)$$

for some function R of λ and the time step h . The stability domain of this method is defined as the following subset of the complex plane [1, 2]:

$$D = \{ (\lambda h) \in \mathbb{C} : |R(\lambda, h)| < 1 \}. \quad (9)$$

When the time step h is such that λh lies in the stability region, the approximate solution decreases to zero, like the exact one, when grows.

BPL is not an iterative scheme. It is however relatively easy to adapt to it the notion of stability domain. For equation (7), we have:

$$F(t, u) = \lambda u \quad \text{and} \quad F_k(u_0, \dots, u_k) = \lambda u_k.$$

Equation (3) permits to compute the coefficients of the time series:

$$u_{k+1} = \frac{\lambda u_k}{k+1}$$

When inserted into series (2), these coefficients lead of course to the Taylor development of the exact solution $e^{\lambda t}$. It is a convergent series.

We carry out two linear stability analysis. The first one is when the solution is approximated by the truncated series at order K , without the Borel summation procedure, and the second one is when the solution is approximated with the BPL scheme. When the summation procedure is not applied, the method is generally called Asymptotic Numerical Method (ANM) [31]. With ANM, we have:

$$u(t_0 + h) = \left(\sum_{k=0}^K \frac{(h\lambda)^k}{k!} \right) u(t_0).$$

Comparing this relation to (8), we define the domain of linear stability, for a given truncature order K as

$$D_{ANM}^K = \left\{ z \in \mathbb{C} \text{ such that } \left| \sum_{k=0}^K \frac{z^k}{k!} \right| \leq 1 \right\}. \quad (10)$$

This domain is plotted in Figure 1 for K from 2 to 10. As can be observed, D_K grows with K . The growth is however rather slow. Let us use the positive number $|D_{ANM}^K|$ defined as follows as a quantification of the size of D_{ANM}^K :

$$|D_{ANM}^K| = \sup \{ d \geq 0 \text{ such that } [-d, 0] \in D_{ANM}^K \}. \quad (11)$$

This quantity increases almost linearly as can be seen in Figure 1. The slope of the curve is about 0.375.

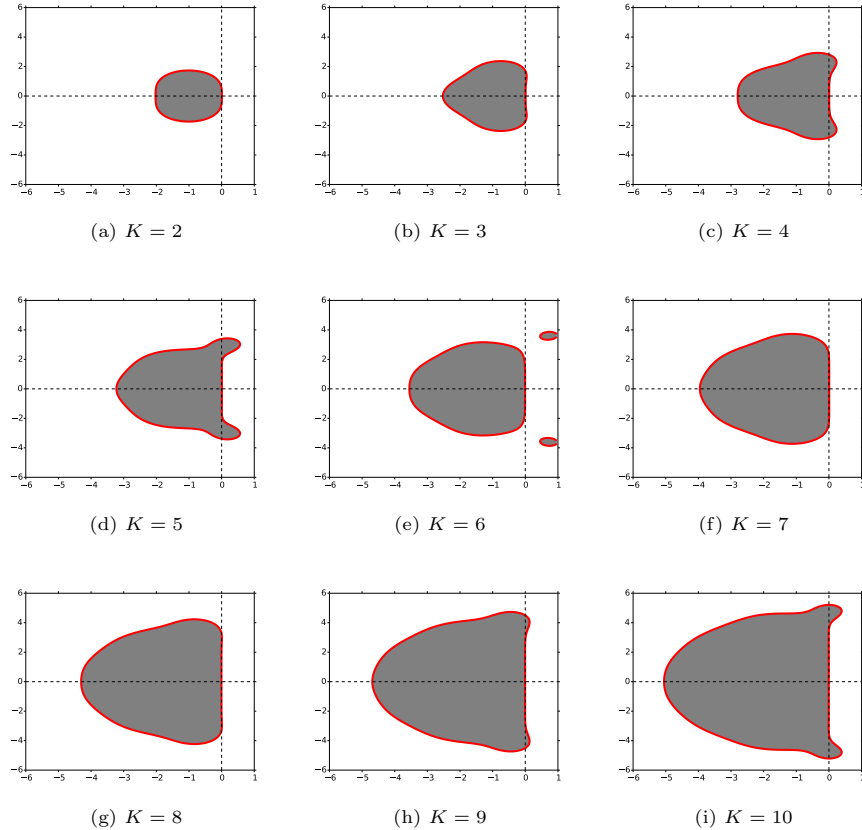


Figure 1: Linear stability regions of the truncated Taylor series approximation (without Borel summation)

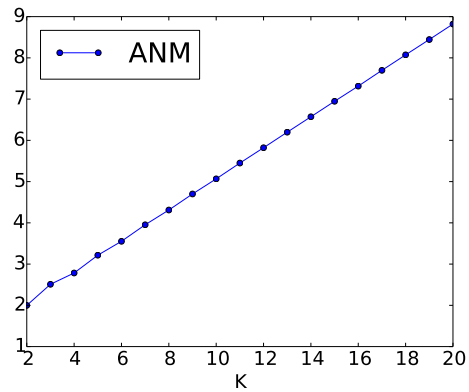


Figure 2: Size $|D_{ANM}^K|$ of the stability region when K grows

In fact, the region D_{ANM}^K coincides with the stability region of an explicit K -th order Runge-Kutta method. The reason to this is that the stability function of an explicit Runge-Kutta method is a truncated Taylor expansion of the exponential function.

We now apply the summation procedure to the series. To make it more concrete, let us set $t_0 = 0$, $u_0 = 1$ and $K = 4$. Like previously, the truncated series solution is

$$\sum_{k=0}^4 \frac{(\lambda t)^k}{k!} = 1 + \frac{\lambda t}{1} + \frac{(\lambda t)^2}{2} + \frac{(\lambda t)^3}{6} + \frac{(\lambda t)^4}{24}. \quad (12)$$

Its Borel transform writes

$$\sum_{k=0}^3 \frac{\lambda^{k+1}}{(k+1)!} \frac{\xi^k}{k!} = \lambda \left(1 + \frac{\lambda \xi}{2} + \frac{(\lambda \xi)^2}{12} + \frac{(\lambda \xi)^3}{144} \right) \quad (13)$$

We take $k_a = 1$ and $k_b = 2$. The $[1/2]$ Padé approximant of (13) is

$$P(\xi) = \lambda \frac{48 + 14\lambda\xi}{48 - 10\lambda\xi + (\lambda\xi)^2}. \quad (14)$$

We then have the following approximated solution of the linear equation (7) with the Borel-Padé-Laplace scheme

$$u(t) \simeq 1 + t \sum_{i=0}^{N_G} P(t\xi_i) \omega_i = 1 + \lambda t \sum_{i=0}^{N_G} P'(\lambda t \xi_i) \omega_i \quad (15)$$

where P' is the rational function

$$P'(z) = \frac{1}{2} \frac{24 + 10z + z^2}{12 - z}. \quad (16)$$

Note that the Padé approximant (14) has no pole on the integration domain (the real positif axis) of the Laplace integral since λ has a negative real part.

The stability region of Borel-Padé-Laplace integrator, for $K = 4$, is

$$D_{BPL}^4 = \left\{ z \in \mathbb{C} \text{ such that } \left| 1 + z \sum_{i=0}^{N_G} P'(z \xi_i) \omega_i \right| \leq 1 \right\}. \quad (17)$$

This region is plotted in Figure 3, with $N_G = 100$ Gauss points, along with the stability regions for other values of K , ranging from 2 to 10. In this Figure, the Padé approximants in Borel space is choosen as closed as possible to the diagonal. More precisely, the degrees of the numerator and denominator are set to

$$K_a = \left\lfloor \frac{K-1}{2} \right\rfloor \quad \text{and} \quad K_b = K - 1 - K_a \quad (18)$$

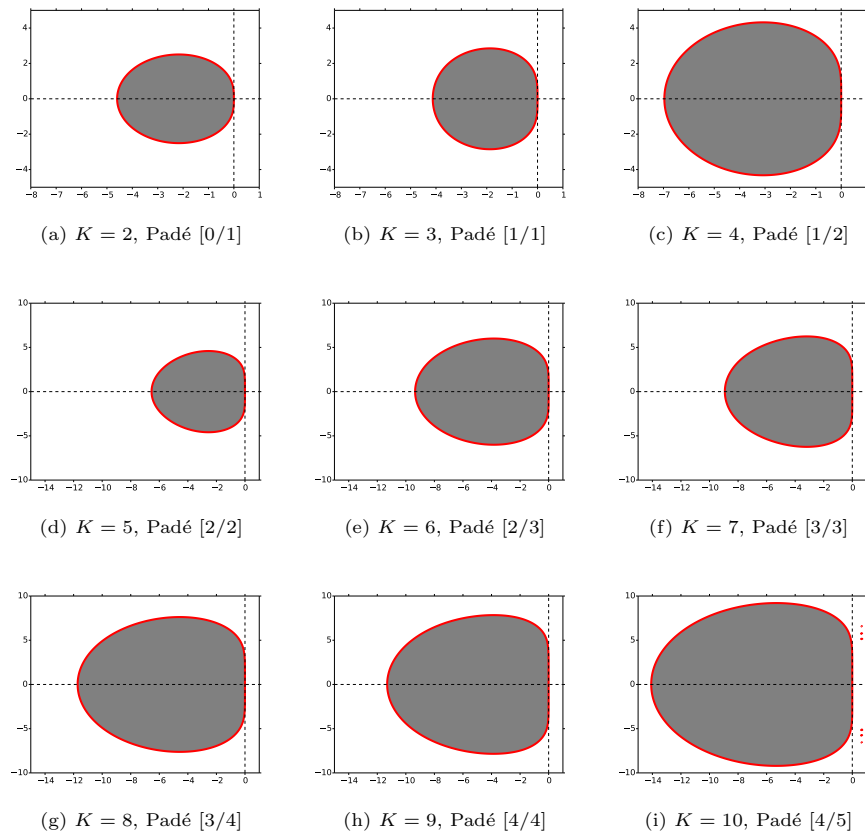


Figure 3: Linear stability regions of Borel-Padé-Laplace integrator with increasing K and with $K_a = \lfloor \frac{K-1}{2} \rfloor$ and $K_b = K - 1 - K_a$.

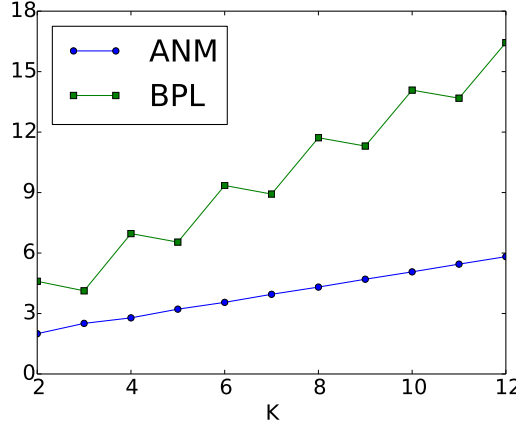


Figure 4: Evolution of $|D_{ANM}^K|$ and $|D_{BPL}^K|$ with K

and are mentioned under each graphic. The symbol $\lfloor \cdot \rfloor$ designates the floor operator. The choice (18) is arbitrary and other choices will be considered later.

As can be seen in Figure 3, the regions do not include the half complex plane with negative real part. Indeed, as an explicit scheme, BPL is not A -stable. However, this figure clearly shows that, for a fixed $K \geq 4$, the stability region of BPL is much bigger than that of the simple truncated series scheme or that of an explicit Runge-Kutta. Note that when $K = 2$, the Borel summation has no effect, and the stability region is the same as in Figure 1a.

Another striking point is that the growth of the stability region with K is not as regular as in the case where the Borel summation is not applied. This is due to the choice of Padé approximant done in (18). However, if we consider either only odd K or only even K , the growth is regular again. In all cases, the overall growth rate is higher than in Figure (1a). Indeed, let us quantify the size of D_{BPL}^K as previously with

$$|D_{BPL}^K| = \sup \{ d \geq 0 \text{ such that } [-d, 0] \in D_{BPL}^K \} \quad (19)$$

The evolution of $|D_{BPL}^K|$ with K is plotted in Figure 4 (along with the evolution of $|D_{ANM}^K|$ for comparison), for K ranging from 2 to 12. The mean slope of the curve of $|D_{BPL}^K|$ is about 0.543.

Since we are in the particular situation where the solution has very fast decreasing Taylor coefficients, only few terms of the series are numerically meaningful. More precisely, the coefficients u'_k of the Borel transformed series are under our machine precision (about $2 \cdot 10^{-16}$) for $k > 11$. So taking $K > 12$ does not bring a substantial amelioration.

These observations demonstrates the importance of the Borel summation procedure, even in a situation where it has not been developed for. Indeed, the summation procedure enlarges very significantly the stability region, even when

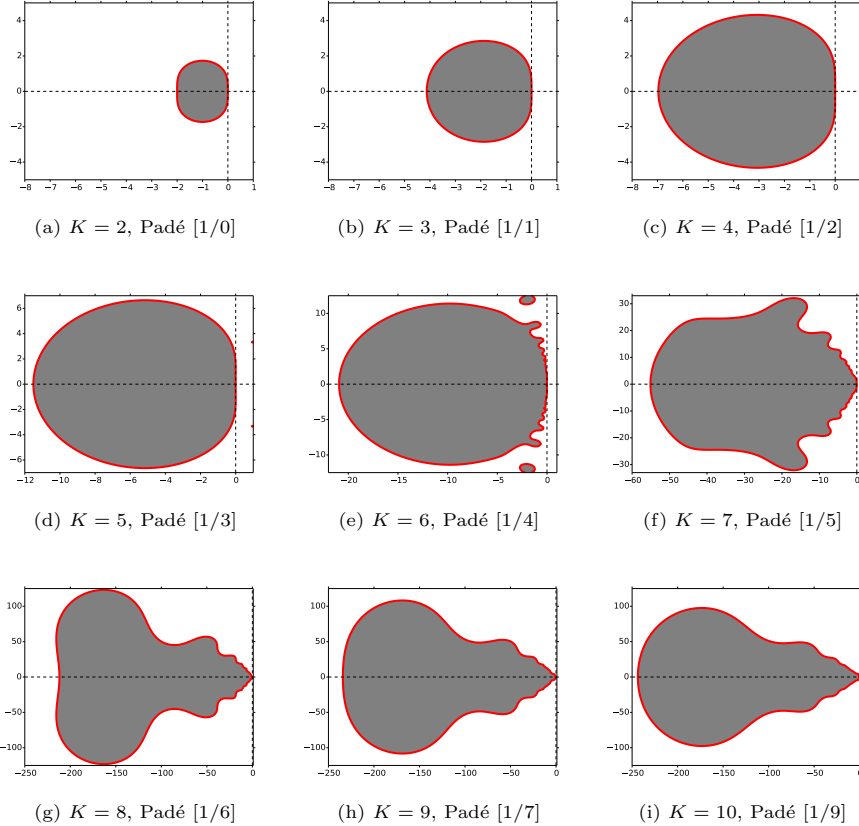


Figure 5: Linear stability regions of Borel-Padé-Laplace integrator with increasing K and fixed $K_a = 1$

the series solution is convergent, with an infinite radius of convergence. This stability region can even be larger if we play with the parameters of the Padé approximants in Borel space. Awaiting a rigorous study of the influence of the choice of K_a and K_b on the stability of BPL, we plot in Figure 5 the evolution of D_{BPL}^K with K when K_a is fixed to 1. As can be observed, the stability domain grows with K and is almost always far larger compared to Figures 1 and 3. The growth rate is also far bigger.

To end up, we would like to analyse graphically the influence of K_a (or K_b) when K is fixed. The stability regions corresponding to $K = 10$ and different Padé degrees are plotted in Figure 6. It can be observed that the stability region grows with the degree K_b of the Padé denominator. When $K_a = 0$ (Figure 6j), BPL tends to be $A(\alpha)$ -stable for some angle α . A theoretical study on the optimal choice of K_a and K_b , which take into account the stability and the precision, would be very interesting but has not been carried out yet.

Note that some of the plotted stability regions are shrunk. Indeed, the

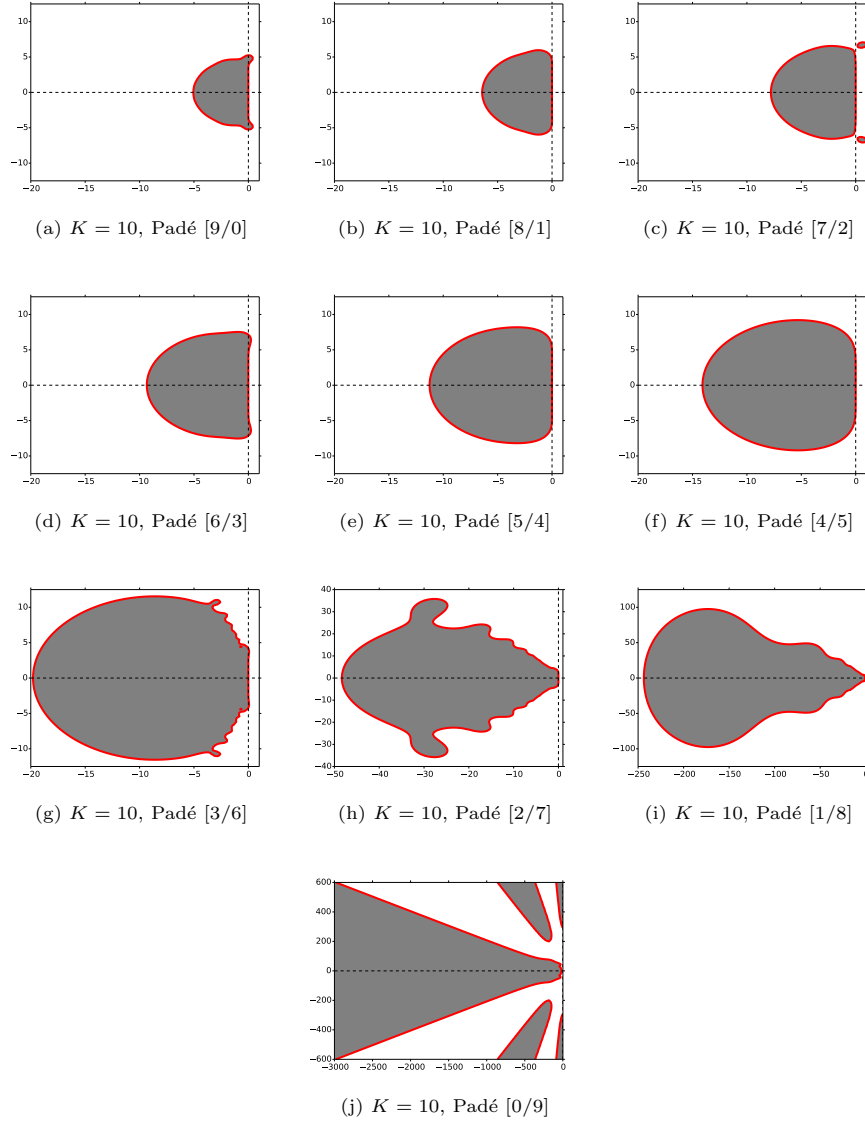


Figure 6: Linear stability regions of Borel-Padé-Laplace integrator for fixed $K = 10$ and decreasing K_a

whole stability regions may contain other parts in the complex plane, but these parts have been excluded from the graphics.

In the next section, the performance of BPL in solving stiff and non-stiff equations is analysed. The coefficients K_a and K_b are chosen as close to each other as possible, as in (18). As seen, it does not correspond to an optimal choice but it will be shown that this is good enough to obtain a very competitive performance in terms of computation time.

As mentioned, all the previous figures were plotted with $N_G = 100$ Gauss points. For $N_G = 20$ and for $N_G = 200$, only small changes have been recorded for Figure 3. So, for the upcoming numerical tests, N_G is set to 20.

4 Numerical performance

Unless otherwise stated, the order K of BPL is set to 10. The degrees of the rational function in the Padé approximant are $K_a = 5$ and $K_b = 4$.

We compare BPL with some classical numerical schemes. Some of them are popular choices for solving stiff equations. More details on them can be found in [1, 2, 3, 4, 32, 33, 12]. These schemes have either a forth or a tenth consistency order and are listed hereafter.

- The 4-th order explicit Runge-Kutta algorithm with a Fehlberg adaptative time step [34, 1], called RK4 hereinafter.
- The 5-stage 10-th order implicit adaptative Gauss-Legendre method which is a Runge-Kutta scheme combined with a Gauss-Legendre quadrature [1], shortened into GAU.
- The 4-step 4-th order implicit backward differentiation formula [35, 1], initiated with RK4, and designated by BDF in this article.
- The 4-th order exponential time differencing method combined with the adaptative Runge-Kutta-Fehlberg method [12]. The pseudo-inversion of the linear operator is carried out with a sigular value decomposition and the evaluation of the matrix exponential is done with a matricial Padé approximation (other possibilities are available in literature). This method is generally called ETDRK4, but will simply be refered to as ETD.

RK4 has been chosen for its popularity and speed in solving non-stiff equations, GAU for its order 10 (the same order as that set for BPL), BDF for its popularity in solving stiff equations and ETD because it is a relatively recent integrator. All of these methods are adaptative. Their precision are driven by a tolerance parameter on the estimated error. All the schemes are coded entirely in python with a fairly equal effort in optimization. The computations are run on a single processor. Each of these schemes may have some good properties (simplicity, ...) and domains where it excells. Our goal is not to make a full comparison of BPL with these schemes. The laters are used simply as reference to situate the

performance of BPL. We focus only on precision, on the size of the time step and on computation time.

We first use these schemes to solve Lotka-Volterra equations.

4.1 Lotka-Volterra equations

Consider a prey-predator system, dynamically governed by the Lotka-Volterra equations [36]:

$$\begin{cases} \frac{du}{dt} = \alpha u - \beta uv, \\ \frac{dv}{dt} = -\delta v + \gamma uv, \end{cases} \quad (20)$$

where u and v are respectively the number of preys and predators in the population, and $\alpha, \beta, \delta, \gamma$ are real positive constants. The reproduction parameter α is the natural (exponential) growth rate of preys in absence of predators whereas δ is the natural decline rate of predators in absence of preys. βv is the mortality rate of prey depending on the the number v of predators and δu is the birth rate of predators depending on the number of prey eaten. It is straight forward to show that system (20) possesses the following first integral:

$$I(u, v) = \beta v + \gamma u - \alpha \ln v - \delta \ln u. \quad (21)$$

We first choose a set of coefficients for which the problem is not stiff.

4.1.1 Non-stiff case

Take an initial population which counts two preys and one predator, that is $u_0 = 2$ and $v_0 = 1$. The reproduction/decline parameters are set to $\alpha = 2/3$ and $\delta = 2$ and the predation parameters to $\beta = 4/3$ and $\gamma = 2$.

For BPL, the coefficients of the time series are determined by the recurrence relation

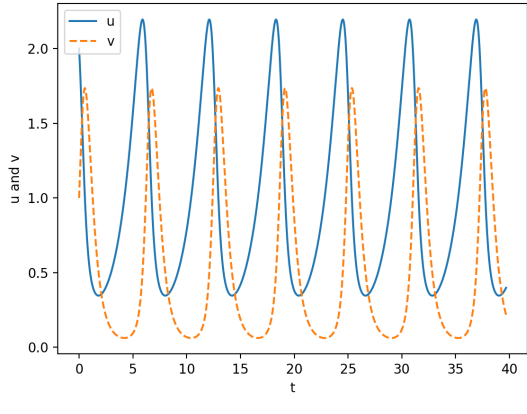
$$\begin{cases} u_{k+1} = \alpha u_k + \beta \sum_{l=0}^k u_l v_{k-l}, \\ v_{k+1} = -\delta v_k + \gamma \sum_{l=0}^k u_l v_{k-l}. \end{cases} \quad (22)$$

The right-hand side of this relation constitutes the function F_k in equation (3). The residue tolerance ϵ of BPL is set such that the mean error on the first integral (21) is about $1.35 \cdot 10^{-7}$ over a simulation time $T = 1000$. The mean or overall error is defined as an approximation of

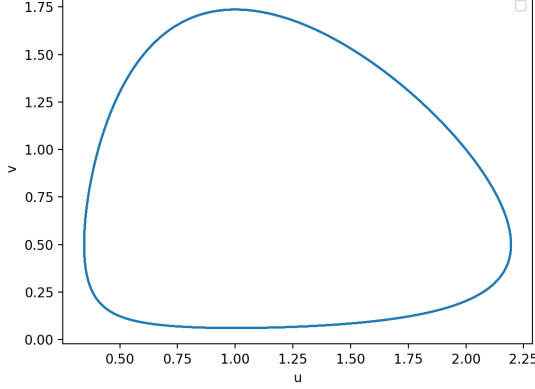
$$\frac{1}{T} \int_0^T \left| I(u(t), v(t)) - I(u(0), v(0)) \right| dt.$$

The approximate solution over 40 seconds is presented in Figure 7. It necessitated 254 iterations. To obtain the smooth graphics in Figure 7, not only

the value of the solution at the discrete times $(t_i)_{i=0,\dots,254}$ but also at some intermediate times $t \in]t_i, t_{i+1}[$. Contrarily to many other schemes, no interpolation method is needed for this. Formula (6) directly provides the approximate solution within each interval $]t_i, t_{i+1}[$.



(a) Time evolution



(b) Trajectory in (u, v) plane

Figure 7: Approximate solution with BPL

The tolerance parameters of BDF, ETD, GAU and RK4 are set such that their a posteriori accuracy are comparable to that of BPL. The mean errors are reported in Table 2. They are around $4 \cdot 10^{-7}$.

Figure 8a shows the evolution of the time steps of the different methods. The solution being periodic, only the evolution over the last 100 seconds are plotted. As can be seen, it is with BPL that the time step is the biggest. Since we are in a non-stiff case, the classical Runge-Kutta method has a good performance

| | BDF | BPL | ETD | GAU | RK4 |
|----------------|----------------------|----------------------|----------------------|----------------------|----------------------|
| Mean error | $5.56 \cdot 10^{-7}$ | $1.35 \cdot 10^{-7}$ | $7.22 \cdot 10^{-7}$ | $4.6 \cdot 10^{-7}$ | $2.38 \cdot 10^{-7}$ |
| Mean time step | $2.42 \cdot 10^{-3}$ | $1.65 \cdot 10^{-1}$ | $2.07 \cdot 10^{-4}$ | $3.70 \cdot 10^{-2}$ | $3.10 \cdot 10^{-2}$ |
| CPU | $5.96 \cdot 10^2$ | 4.32 | $9.34 \cdot 10^2$ | $4.50 \cdot 10^1$ | 4.96 |

Table 2: Error on the first integral and CPU time

and competes with the 10 order Gauss scheme in terms of time step. Figure 8b represents the same data as Figure 8a but with a logarithmic scale in ordinate. It shows that the time step of BPL is about 60 times bigger than that of BDF and about 80 times bigger than that of ETD. It is confirmed in mean in Table 2. As for CPU time, the two explicit integrators, BPL and RK4, have a comparable performance (see Table 2). They need about 10 times less computation time than GAU and at least 100 times less than BDF and ETD.

In a second test, each scheme is run with multiple values of the (residue or estimated error) tolerance. The mean time step is plotted in Figure 9 against the overall precision. This figure clearly shows that, amongst the considered schemes, BPL has always the biggest mean time step, whatever the precision. This mean time step is about 6.6 times bigger than that of the Gauss scheme with the same order for an error around $3 \cdot 10^{-9}$. This big time step traduces in a faster computation. Indeed, as can be noticed in Figure 10, BPL requires much less CPU time than GAU, for comparable precisions. Only RK4 is faster than BPL for a medium or a low precision. But when a high precision is required, BPL tends to be more interesting.

4.1.2 Increasing the stiffness ratio

We now examine the behaviour of the schemes when the stiffness ratio varies. The stiffness ratio r is defined as the spectral condition number of the linear part of equations (20), that is

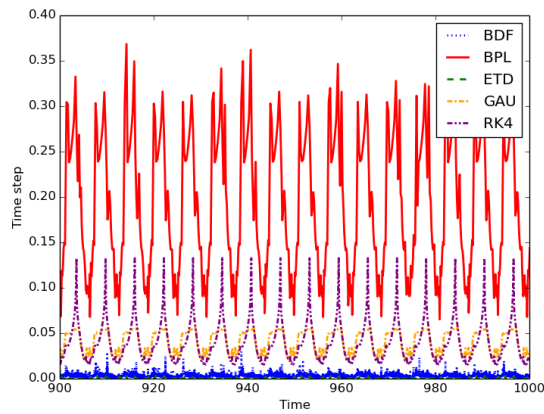
$$r = \frac{\max(\alpha, \delta)}{\min(\alpha, \delta)} \quad (23)$$

since α and δ are positive reals. In fact, r appears naturally if equations (20) are adimensionalized with the variables

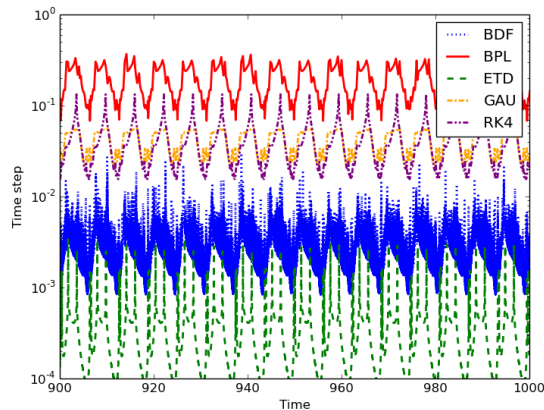
$$u^* = \frac{\gamma u}{\delta}, \quad v^* = \frac{\beta v}{\alpha}, \quad t^* = \alpha t.$$

Indeed, equations (20) can be written as follows:

$$\begin{cases} \frac{du^*}{dt^*} = & u^* - u^*v^*, \\ \frac{dv^*}{dt^*} = & r(-v^* + u^*v^*). \end{cases} \quad (24)$$



(a) Linear scales



(b) Semi-logarithmic scale

Figure 8: Non-stiff Lotka-Volterra. Evolution of time step

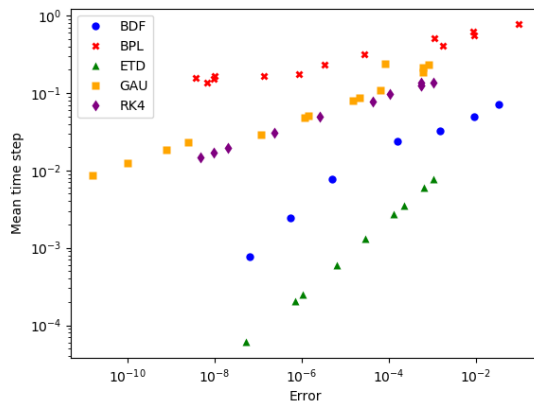


Figure 9: Non-stiff Lotka-Volterra. Evolution of the mean time step with the mean error

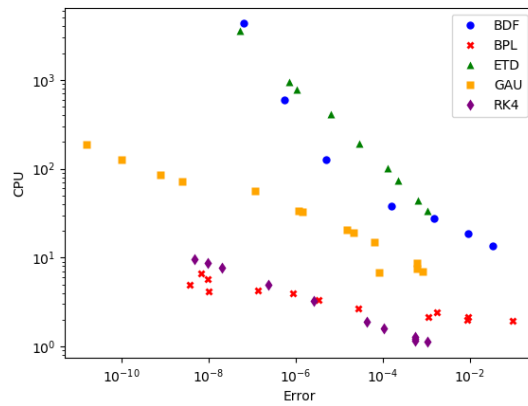


Figure 10: Non-stiff Lotka-Volterra. Evolution of CPU with the mean error

All the parameters of the equations are kept at the same value as before, except δ which is increased. In particular, we will always have $\delta > \alpha$ and $r = \delta/\alpha$. As before, simulations are run with multiple values of the (residue or estimated error) tolerance until 1000 seconds. The error on the first integral and the CPU time are recorded and plotted hereafter.

For a moderate stiffness ratio $r = 8$, Figure 11 shows that RK4 and BPL compete in terms of CPU time, even if BPL indicates a slight advantage for high precision simulations. It can also be stated in this figure that GAU can provide a very precise solution, due to its high order, but with a higher cost than BPL. BDF and ETD are much more expensive than the other schemes.

For $r = 16$, we have approximately the same picture, except that BPL becomes more interesting than RK4 even for moderate precisions. This can be observed in Figure 12.

When the stiffness ratio is set to a high value $r = 32$, the situation changes significantly. First, as can be seen in Figure 13, RK4 cannot reach very high precision any longer, compared to BPL. The precision that can be achieved with GAU is still very high but not as high as with $r = 16$. ETD also loses precision. Only BPL is able to maintain the same precision as previously.

Concerning the numerical cost, the augmentation of CPU time needed by BPL and ETD is very small compared to that of GAU.

Lastly, BDF does not appear in Figure 13. Indeed, although it is a popular method for stiff equations, it fails with $r = 32$. It diverges as soon as t reaches some seconds. This behaviour has also been observed with the optimized BDF solver of the python `scipy` package, with the optimized BDF solver of Scilab, and with the option `CVODE_BDF` of the package `Sundials` of Julia language.

For $r = 64$, ETD also fails. As remarked in Figure 14, RK4 gives moderately precise solutions, and even wrong solutions for some values of the predicted error tolerance. Indeed, even for very small value of the tolerance, the overall error may be bigger than one. Figure 14 also shows that the precision of GAU seems to stagnate around $2.6 \cdot 10^{-4}$. Only BPL can provide highly accurate solutions. Moreover, its CPU cost is very small compared to that of GAU.

At last, with $r = 128$, the Gauss method also fails. This behaviour has as well been observed with the Gauss solver of the Matlab package `numeric::odesolve`. For this value of the stiffness ratio, RK4 cannot give an accurate solution any longer, whereas with BPL, the error can be as small as $7.4 \cdot 10^{-10}$ (see Figure 15).

These numerical experiments show that BPL is a serious alternative method for stiff problems. First, its arbitrary high order enables to get highly accurate solutions. With Lotka-Volterra equations, it never fails for values of r up to 128. Moreover, its cost is generally much smaller than that of the other methods, due to its explicit property.

The previous tests show the performance of BPL for the resolution of stiff and non-stiff ODE's. In the next subsection, we examine its efficiency in solving partial differential equations.

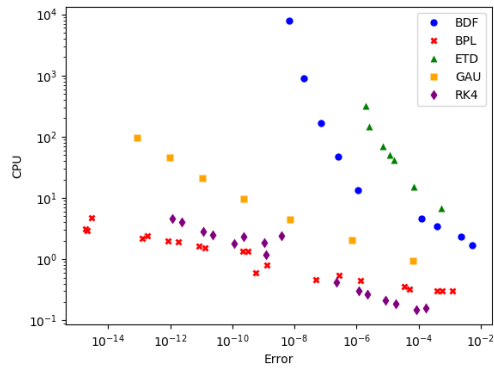


Figure 11: Lotka-Volterra. Stiffness ratio $r = 8$

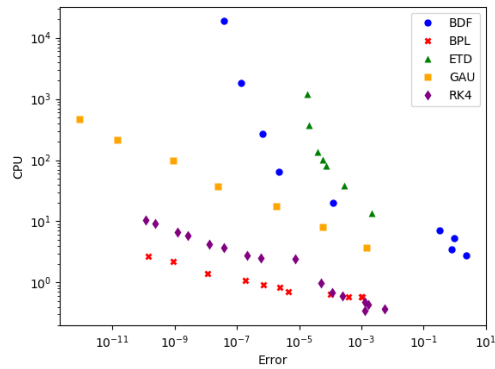


Figure 12: Lotka-Volterra. Stiffness ratio $r = 16$

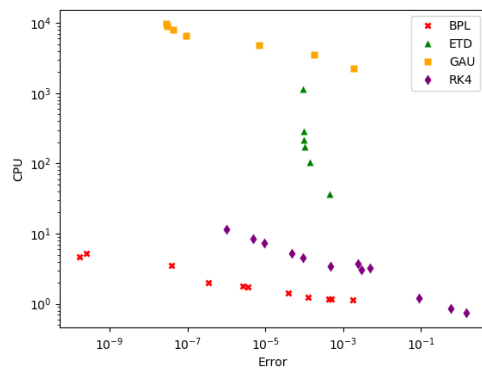


Figure 13: Lotka-Volterra. Stiffness ratio $r = 32$

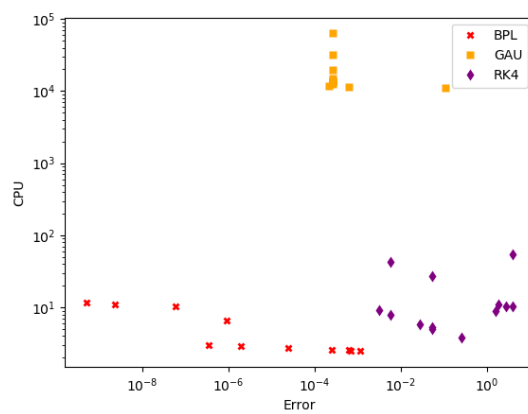


Figure 14: Lotka-Volterra. Stiffness ratio $r = 64$

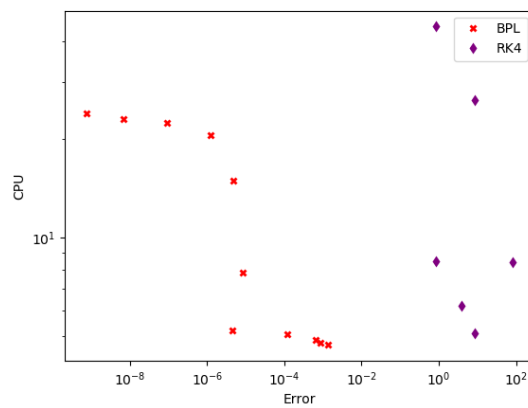


Figure 15: Lotka-Volterra. Stiffness ratio $r = 128$

4.2 Korteweg-de-Vries equation

In this subsection, we consider the Korteweg-de-Vries equation (KdV)

$$\frac{\partial u}{\partial t} + c_0 \frac{\partial u}{\partial x} + \beta \frac{\partial^3 u}{\partial x^3} + \frac{\alpha}{2} \frac{\partial u^2}{\partial x} = 0 \quad (25)$$

which models waves on shallow water surfaces [37]. In this equation, the linear propagation velocity c_0 , the non-linear coefficient α and the dispersion coefficient β are positive constants, linked to the gravity acceleration g and the mean depth d of the water by:

$$c_0 = \sqrt{gd}, \quad \alpha = \frac{3}{2} \sqrt{\frac{g}{d}}, \quad \beta = \frac{d^2 c_0}{6}. \quad (26)$$

In order to focus on the performance of the time integrators, we choose a high order scheme, namely a spectral method, for the space discretization. The solution is assumed to be periodic with period X in space, and integrable. It is approximated by its truncated Fourier series:

$$u(x, t) \simeq \sum_{|m| \leq M} \hat{u}^m(t) e^{im\omega x}, \quad (27)$$

where $M \in \mathbb{N}$ and $\omega = \frac{2\pi}{X}$. The injection of equation (27) into (25) leads to a $(2M + 1)$ -dimensional ODE

$$\frac{d\hat{u}}{dt} = A\hat{u} + N(\hat{u}) \quad (28)$$

where the array \hat{u} contains the unknowns \hat{u}^m , A is a diagonal matrix with diagonal entries

$$A_m^m = -c_0 i\omega m + i\beta\omega^3 m^3$$

and $N(\hat{u})$ is a non-linear array containing convolution terms:

$$N(\hat{u}) = -\frac{1}{2} i\alpha m \omega \hat{u} * \hat{u}.$$

Convolution operations are performed in physical space and the standard dealiasing 3/2 rule is applied.

With BPL, each component $\hat{u}^m(t)$ of the Fourier coefficient array $\hat{u}(t)$ is decomposed into a time series

$$\hat{u}^m(t) = \sum_{k=0}^K \hat{u}_k^m t^k. \quad (29)$$

The series coefficients are computed explicitly as follows:

$$\hat{u}_{k+1} = \frac{1}{k+1} \left[(-c_0 i\omega m + i\beta\omega^3 m^3) \hat{u}_k - \frac{1}{2} i\alpha m \omega \sum_{l=0}^k \hat{u}_n * \hat{u}_{k-l} \right]. \quad (30)$$

| <i>D</i> | BDF | BPL | ETD | GAU | RK4 |
|-----------------|----------------------|----------------------|----------------------|----------------------|----------------------|
| 64 | $1.09 \cdot 10^{-1}$ | $3.71 \cdot 10^{-4}$ | $2.92 \cdot 10^{-3}$ | $5.11 \cdot 10^{-3}$ | $1.83 \cdot 10^{-3}$ |
| 128 | $1.08 \cdot 10^{-2}$ | $3.54 \cdot 10^{-4}$ | $3.27 \cdot 10^{-3}$ | $5.81 \cdot 10^{-3}$ | $1.69 \cdot 10^{-3}$ |
| 256 | — | $3.61 \cdot 10^{-4}$ | $3.66 \cdot 10^{-3}$ | $4.00 \cdot 10^{-3}$ | $1.23 \cdot 10^{-3}$ |
| 512 | — | $3.17 \cdot 10^{-4}$ | $4.11 \cdot 10^{-3}$ | $2.65 \cdot 10^{-3}$ | $6.50 \cdot 10^{-4}$ |

Table 3: KdV. Overall error

For the simulations, the initial condition is the periodic prolongation of the function

$$u_0(x) = U \operatorname{sech}^2(\kappa x), \quad x \in \left[-\frac{X}{2}, \frac{X}{2}\right], \quad (31)$$

U being a constant and $\kappa = \sqrt{\frac{3U}{4d^3}}$. The corresponding exact solution is the traveling wave

$$u(x, t) = u_0(x - ct). \quad (32)$$

with $c = c_0 \left(1 + \frac{U}{2d}\right)$. We take $X = 24\pi$, $d = 2$, $g = 10$ and $U = \frac{1}{2}$. The solution is periodic in time, with a period $T \simeq 14.986$ s.

We use $D = 2M$ to indicate the size of the system, instead of the dimension $2M + 1$ of equation (28). The simulations are run over one period, for some values of D between 64 and 512.

Its is hard to calibrate the tolerance parameters of all the schemes to have the same (a posteriori) overall error at each value of D . So, this calibration has not been done. Instead, we have ensured that we are demanding more accuracy to BPL that to the other methods, in order not to overestimate the performance of BPL. The overall error are recorded in Table 3. The error reported in this table is an approximation of

$$\int_0^T \frac{\|u_{\text{computed}}(t) - u_{\text{exact}}(t)\|}{\|u_{\text{exact}}(t)\|} dt. \quad (33)$$

The evolution of the computation time of each scheme is plotted in Figure 16. It can be seen there that BDF requires a very high cost for $D = 128$, despite the very low precision (second column of Table 3). As a consequence, it has not been used for higher values of D .

Figure 16 also shows that, among the considered schemes, RK4 is the fastest for (non-stiff) small-sized problems, for the given precisions. But for high degrees of freedom, BPL becomes the most interesting in terms of computational term. BPL also has the smallest slope.

Figure 17 indicates that BPL has a very big mean time step compared to the other schemes, whatever the size of the problem. It is also striking that the mean time step does not vary very much with the size of the problem. However, BPL is not the only schemes which presents this characteristics since the ETD has the same behavior, but with much smaller time steps.

The big time step of BPL is of a great importance in its performance. Indeed, the CPU time spend at each time step is very high with BPL than with

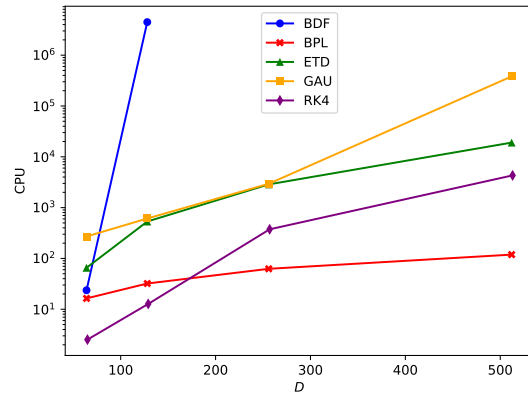


Figure 16: KdV. Evolution of the computation time with the size D of the problem

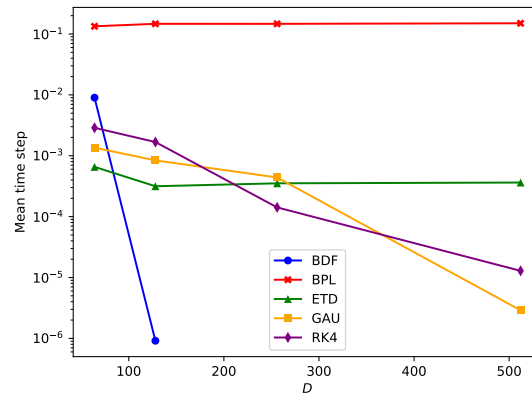


Figure 17: KdV. Evolution of the mean time step with the size D of the problem

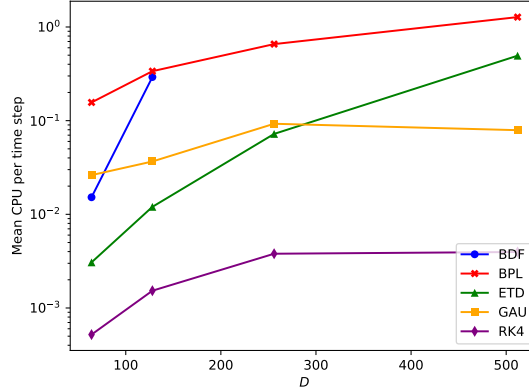


Figure 18: KdV. Mean CPU time per time step

the other schemes, as can be stated in Figure 18. One reason to this is the evaluation of the residue in step 6 of the algorithm presented in section 2.2. This evaluation is done multiple times at each time step to decide if the solution is still precise enough. Another precision evaluation is desirable, but not available yet. Fortunately, this expensive precision evaluation is largely counter-balanced by big time steps.

In all of the previous simulations, the order K of the time series in BPL was set to 10. In our last test, the effect of K on the performance of BPL is analysed. For this, the size of the problem is set to $D = 128$. A residue tolerance $\epsilon = 1 \cdot 10^{-4}$ is chosen. Figure 19 shows the L^1 relative error (defined in equation (33)) over one period. This figure reveals a fluctuation of the error according to the parity of K . Note that such fluctuation is not uncommon when manipulating truncated series. Moreover, the parity of K intervenes in the choice of the Padé approximants in Borel space. Indeed, when K is odd, the numerator and the denominator of the Padé approximant have the same degree; and when K is even, the denominator has a higher degree than the numerator (see choice in equation (18)). Figure 19 however tells us that globally, the accuracy increases with the order K of the series, for a fixed value of the residue tolerance.

The mean time step has also a globally increasing tendency with K as can be seen in Figure 20, passing from $\Delta t_{mean} = 0.0256$ for $K = 4$ to $\Delta t_{mean} = 0.156$ when $K = 14$. As a consequence, the CPU time decreases with K , as can be noted in Figure 21. These results tend to indicate that high values of K accelerate the computation.

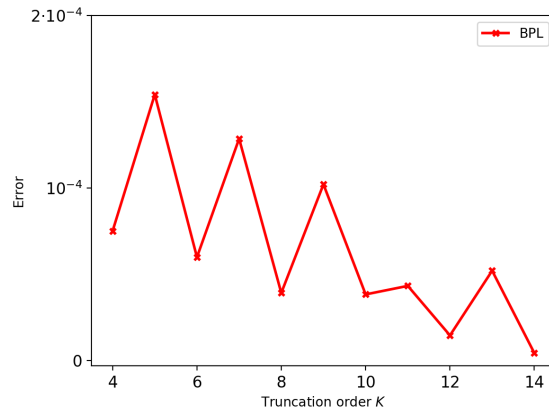


Figure 19: KdV. Evolution of the error with K

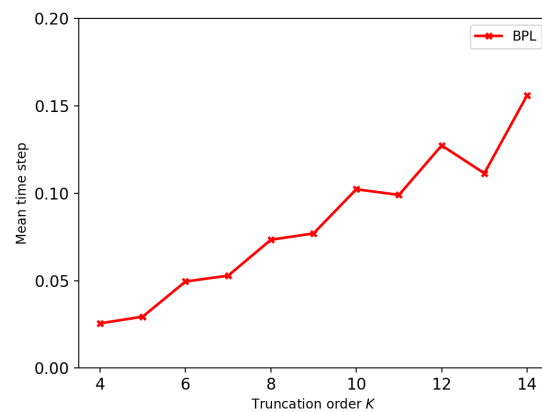


Figure 20: KdV. Evolution of the mean time step with K

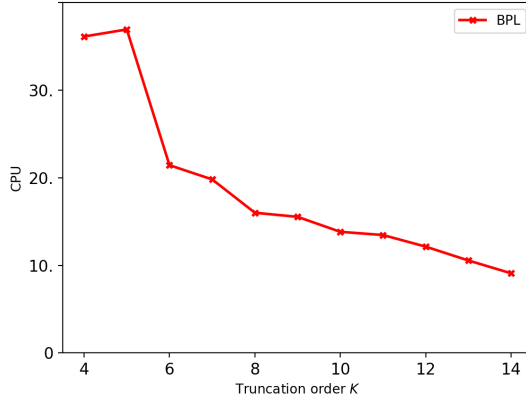


Figure 21: KdV. Evolution of the computation time with K

5 Conclusion

In this article, we studied the linear stability of the Borel-Padé-Laplace integrator. It has been shown that if the summation procedure is not applied, the scheme has the same linear stability domain as an explicit Runge-Kutta integrator. But when the summation is carried out, the linear stability domain enlarges very significantly, even if the solution series is convergent. It has been noticed that the size of this domain increases with the order of truncature of the solution series. We also saw that the choice of Padé approximants in Borel space has a substantial impact on the size of the linear stability domain.

Even if BPL is not A -stable, it has been shown that this scheme is more efficient than many explicit and many implicit ones, in solving stiff problems. It runs without any particular difficulty for a wide range of stiffness number. Due to its high order, it can reach very high precisions even when the stiffness number is high. Moreover, its explicit property makes it very fast compared to the other integrators.

Numerical tests on non-stiff Lotka-Volterra and on Korteweg-de-Vries equations showed that for small-size systems, the popular 4-th order Runge-Kutta method has a comparable speed than BPL when only a moderate precision is needed. But when high precision is required BPL becomes more interesting. It is even more true when the size of the system is big.

It is worth to notice that increasing the approximation order of BPL does not necessitate any programming effort. One has simply to raise the cut-off parameter K of the series, without changing anything else in the algorithm. As could be observed in the last part of the article, the higher this value is, the faster BPL is.

Despite its speed, one optimization should be brought to the algorithm of BPL. Indeed, a numerical test with Korteweg-de-Vries equation showed that a

BPL time step is rather expensive, due among others to many evaluations of the residue. A less expensive quality evaluation should be developed. This should increase the speed of the scheme.

To obtain the previous results, the computation was done on a single processor. But note that BPL also presents some advantage regarding parallelisation. Indeed, the summation algorithm can be done component-wise, letting the computation to be shared between many processors.

In this paper, only the computational aspects of BPL are discussed. The founding theory was skipped. Yet, some optimizations may be brought to the algorithm with help of theoretical considerations. For instance, a theoretical study of the equation may be helpful to determine the actual Gevrey order (which was set to one in this article). However, it is conceivable to evaluate numerically this Gevrey order from the coefficients of the series. A theoretical study of the equation may also help to find a better (than the real positive semi-line) integration direction in the Laplace transform.

Parler des tests dans le livre de Hairer, Geometric numerical integration, structure preserving ...

References

- [1] E. Hairer and G. Wanner. *Solving Ordinary Differential Equations II: Stiff and Differential-Algebraic Problems*. Springer Series in Computational Mathematics. Springer-Verlag Berlin Heidelberg, 2nd edition, 1996.
- [2] A. Iserles. *A first course in the numerical analysis of differential equations*. Cambridge University Press, 1996.
- [3] J.C. Butcher. *Numerical Methods for Ordinary Differential Equations*. J. Wiley & Sons, Ltd., 2003.
- [4] J.D. Lambert. *Numerical Methods for Ordinary Differential Systems: The Initial Value Problem*. J. Wiley & Sons, Ltd., 1991.
- [5] J.G. Verwer. Explicit runge-kutta methods for parabolic partial differential equations. *Applied Numerical Mathematics*, 22(1):359 – 379, 1996.
- [6] A. Friedli. Verallgemeinerte Runge-Kutta Verfahren zur Lösung steifer Differentialgleichungssysteme. In Bulirsch, Grigorieff, and Schröder, editors, *Numerical Treatment of Differential Equations, Oberwolfach 1976*, pages 35–50. Springer Berlin Heidelberg, 1978.
- [7] P. Norsett. An a-stable modification of the adams-bashforth methods. In J. Li. Morris, editor, *Conference on the Numerical Solution of Differential Equations, Dundee/Scotland*, pages 214–219. Springer Berlin Heidelberg, 1969.

- [8] P.J. van der Houwen and J.G. Verwer. Generalized linear multistep methods, 1 : Development of algorithms with zero-parasitic roots. *Stichting Mathematisch Centrum. Numerieke Wiskunde*, 74(10):1–16, 1974.
- [9] J. Certaine. The solution of ordinary differential equations with large time constants. *Mathematical methods for digital computers*, pages 128–132, 1960.
- [10] M. Hochbruck and A. Ostermann. Exponential Runge–Kutta methods for parabolic problems. *Applied Numerical Mathematics*, 53(2):323 – 339, 2005.
- [11] M. Hochbruck and A. Ostermann. Exponential integrators. *Acta Numerica*, 19:209–286, 2010.
- [12] S. Cox and P. Matthews. Exponential time differencing for stiff systems. *Journal of Computational Physics*, 176(2):430 – 455, 2002.
- [13] E. Borel. *Leçons sur les séries divergentes*. Gauthier-Villars, 1901.
- [14] D. Lutz, M. Miyake, and R. Schäfke. On the borel summability of divergent solutions of the heat equation. *Nagoya Mathematical Journal*, 154:1–29, 1999.
- [15] G. Lysik. Borel summable solutions of the Burgers equation. *Annales Polonici Mathematici*, 95:187–197, 2009.
- [16] O. Costin and S. Tanveer. Borel summability of Navier-Stokes equation in \mathbb{R}^3 and small time existence. *ArXiv Mathematics e-prints*, dec 2006.
- [17] F. Dyson. Divergence of perturbation theory in quantum electrodynamics. *Physical Review*, 85:631–632, 1952.
- [18] I. Suslov. Divergent perturbation series. *Journal of Experimental and Theoretical Physics*, 100(6):1188–1233, 2005.
- [19] G. Kontopoulos. *Order and chaos in dynamical astronomy*. Astronomy and astrophysics library. Springer, Berlin, Heidelberg, New York, 2002.
- [20] J. Thomann. Formal and numerical summation of formal power series solutions of ODE’s. Technical report, CIRM Luminy, 2000.
- [21] D. Razafindralandy and A. Hamdouni. Time integration algorithm based on divergent series resummation, for ordinary and partial differential equations. *Journal of Computational Physics*, 236:56–73, 2013.
- [22] A. Deeb, A. Hamdouni, E. Liberge, and D. Razafindralandy. Borel-Laplace summation method used as time integration scheme. *ESAIM: Proceedings and Surveys*, 45:318–327, 2014.
- [23] A. Deeb, A. Hamdouni, and D. Razafindralandy. Comparison between Borel-Padé summation and factorial series, as time integration methods. *Discrete and Continuous Dynamical Systems - Serie S*, 9(2):393–408, 2016.

- [24] J.-P. Ramis. Poincaré et les développements asymptotiques (Première partie). *Gazettes des Mathématiques*, 133, Juillet 2012.
- [25] J.-P. Ramis. Les développements asymptotiques après Poincaré : continuité et... divergences. *Gazettes des Mathématiques*, 134, octobre 2012.
- [26] O. Costin. *Asymptotics and Borel Summability*. Monographs and Surveys in Pure and Applied Mathematics. CRC Press, 2008.
- [27] C. Brezinski. Rationnal approximation to formal power serie. *Journal of Approximation Theory*, 25(4):295–317, 1979.
- [28] C. Brezinski and J. Van Iseghem. Padé approximations. In P. G. Ciarlet and J. L. Lions, editors, *Handbook of Numerical Analysis*, volume 3, pages 47 – 222. Elsevier, 1994.
- [29] A. Stroud and D. Secrest. *Gaussian quadrature formulas (without numerical tables)*. Prentice-Hall, 1966.
- [30] P. Gonnet, S. Güttel, and L. Trefethen. Robust Padé approximation via SVD. *SIAM Review*, 51(1):101–117, 2013.
- [31] B. Cochelin, N. Damil, and M. Potier-Ferry. *Méthode asymptotique numéorique*. Methodes numériques. Hermès Lavoissier, 2007.
- [32] U. Ascher and L. Petzold. *Computer Methods for Ordinary Differential Equations and Differential-Algebraic Equations*. SIAM, 1998.
- [33] R. J. LeVeque. *Finite Difference Methods for Ordinary and Partial Differential Equations*. Other Titles in Applied Mathematics. SIAM, 2007.
- [34] E. Fehlberg. Klassische Runge-Kutta-Formeln vierter und niedrigerer Ordnung mit Schrittweiten-Kontrolle und ihre Anwendung auf Wärmeleitungsprobleme. *Computing*, 6(1):61–71, Mar 1970.
- [35] C. F. Curtiss and J. O. Hirschfelder. Integration of stiff equations. *Proceedings of the National Academy of Sciences of the United States of America*, 38(3):235–43, 1952.
- [36] J. Hofbauer and K. Sigmund. *The Theory of Evolution and Dynamical Systems: Mathematical Aspects of Selection*. London Mathematical Society Student Texts. Cambridge University Press, 1988.
- [37] D. Korteweg and G. de Vries. On the change of form of long waves advancing in a rectangular canal, and on a new type of long stationary waves. *Philosophical Magazine*, 39(240):422–443, 1895.